Journal of Sound and Vibration (2001) **239**(3), 467–488
doi:10.1006/jsvi.2000.3143, available online at http://www.idealibrary.com on IDEAL®

MECHANICAL AND THERMAL SOURCES IN A MICROPOLAR GENERALIZED THERMOELASTIC MEDIUM

R. KUMAR AND S. DESWAL

Department of Mathematics, Kurukshetra University, Kurukshetra 136 119, *Haryana, India.*
E-mail: vidya.kuk.ernet.in

(*Received* 27 *January* 2000, *and in final form* 9 *June* 2000)

The disturbance due to mechanical and thermal sources in a homogeneous, isotropic, micropolar generalized thermoelastic half-space is investigated by the use of Laplace–Fourier transform technique. The analytical expressions of displacement components, normal force stress, tangential force stress and temperature field so obtained have been inverted by using a numerical technique. Numerical results are presented graphically for a magnesium crystal like material.

1. INTRODUCTION

The linear theory of elasticity is of paramount importance in the stress analysis of steel, which is the most common engineering structural material. To a lesser extent linear elasticity describes the mechanical behaviour of other common solid materials, e.g., concrete, wood and coal. However, this theory does not apply to the behaviour of many of the new synthetic materials of the elastomer and polymer type, e.g., polymethylmethacrylate (perspex), polythylene, polyvinyl chloride.

Modern engineering structures are often made up of materials possessing an internal structure. Polycrystalline materials, materials with fibrous or coarse grain structure come in this category. Classical elasticity is inadequate to represent the behaviour of such materials. The analysis of such materials requires incorporating the theory of oriented media. "Micropolar elasticity" termed by Eringen [1] is used to describe the deformation of elastic media with oriented particles. A micropolar continuum is a collection of interconnected particles in the form of small rigid bodies undergoing both translational and rotational motions. Typical examples of such materials are granular media and multimolecular bodies, whose microstructures act as an evident part in their macroscopic responses. The physical nature of these materials needs an asymmetric description of deformation, while theories for classical continua fail to accurately predict their physical and mechanical behaviour. For this reason, micropolar theories were developed by Eringen [1–3] for elastic solids, fluids and further for non-local polar fields and are now universally accepted.

The coupled theory of thermoelasticity has been extended by including the thermal relaxation time in the constitutive equations by Lord and Shulman (L–S) [4] and Green and Lindsay (G–L) [5]. These new theories eliminate the paradox of infinite velocity of heat propagation and are termed as generalized theories of thermoelasticity. In view of the experimental evidence available in favour of finiteness of heat propagation speed,

0022-460X/01/030467 + 22 $35.00/0

generalized thermoelasticity theories are supposed to be more realistic than the conventional theory in dealing with practical problems involving very large heat fluxes and/or short time intervals, like those occurring in laser units and energy channels. Recently, Green and Naghdi (G–N) [6–8] proposed a new generalized thermoelasticity theory by including the "thermal-displacement gradient" among the constitutive variables that permit treatment of a much wider class of heat flow problems. An important feature of this theory, which is not present in other thermoelasticity theories, is that this theory does not accommodate dissipation of thermal energy.

The linear theory of micropolar thermoelasticity was developed by extending the theory of micropolar continua to include thermal effects by Eringen [9] and Nowacki [10]. Different authors [11–14] discussed different problems in micropolar elasticity/micropolar theory of thermoelasticity.

The purpose of the present paper is to determine the normal displacement, normal force stress, tangential couple stress and temperature distribution in a homogeneous, isotropic, micropolar generalized thermoelastic half-space due to instantaneous mechanical and thermal sources by applying integral transform techniques. Numerical techniques have been used to invert the integral transforms. The components of stresses, displacements and temperature field are calculated for the mechanical and thermal impulses. Applications of the present problem may also be found in the field of steel and oil industries. The present problem is also useful in the field of geomechanics, where the interest is about the various phenomenon occurring in the earthquakes and measuring of displacements, stresses and temperature field due to the presence of certain sources.

2. FORMULATION OF THE PROBLEM

A homogeneous, isotropic, micropolar generalized thermoelastic solid occupying the half space is considered in an undisturbed state and initially at uniform temperature T_0. The rectangular Cartesian co-ordinates are introduced having origin on the surface $z = 0$ and z-axis pointing vertically into the medium. An instantaneous normal point mechanical or thermal source is assumed to be acting at the origin of the rectangular Cartesian co-ordinates. Let $T(x, z, t)$ be the change in temperature of the medium at any time.

Following Eringen [15], Lord and Shulman [4] and Green and Lindsay [5], the field equations and stress–strain temperature relations in micropolar generalized thermoelastic solid without body forces, body couples and heat sources can be written as

$$(\lambda + \mu)\nabla(\nabla\cdot\mathbf{u}) + (\mu + K)\,\nabla^2\mathbf{u} + K\nabla x\boldsymbol{\phi} - \nu\left(1 + t_1\frac{\partial}{\partial t}\right)\nabla T = \rho\,\frac{\partial^2\mathbf{u}}{\partial t^2}, \tag{1}$$

$$(\alpha + \beta + \gamma)\nabla(\nabla\cdot\boldsymbol{\phi}) - \gamma\nabla x(\nabla x\boldsymbol{\phi}) + K\nabla x\mathbf{u} - 2K\boldsymbol{\phi} = \rho j\,\frac{\partial^2\boldsymbol{\phi}}{\partial t^2}, \tag{2}$$

$$K^*\nabla^2 T = \rho C^*\left(\frac{\partial T}{\partial t} + t_0\frac{\partial^2 T}{\partial t^2}\right) + \nu T_0\left(\frac{\partial}{\partial t} + \Xi t_0\frac{\partial^2}{\partial t^2}\right)\nabla\cdot\mathbf{u} \tag{3}$$

and

$$t_{ij} = \lambda u_{r,r}\delta_{ij} + \mu(u_{i,j} + u_{j,i}) + K(u_{j,i} - \varepsilon_{ijr}\,\phi_r) - \nu\left(T + t_1\frac{\partial T}{\partial t}\right)\delta_{ij}, \tag{4}$$

$$m_{ij} = \alpha\phi_{r,r}\delta_{ij} + \beta\phi_{i,j} + \gamma\phi_{j,i}, \tag{5}$$

where λ, μ, K, α, β, γ are material constants, ρ is density, j is the microinertia, K^* is the coefficient of thermal conductivity, $\nu = (3\lambda + 2\mu + K)\ \alpha_t$, α_t is the coefficient of linear thermal expansion, C^* is the specific heat at constant strain, t_0, t_1 are the thermal relaxation times, $\mathbf{u}$ the displacement vector, $\boldsymbol{\phi}$ the microrotation vector. For the Lord–Shulman (L–S) theory $t_1 = 0$, $\Xi = 1$ and for Green–Lindsay (G–L) theory $t_1 > 0$ and $\Xi = 0$. The thermal relaxations t_0 and t_1 satisfy the inequality $t_1 \geqslant t_0 \geqslant 0$ for the G–L theory only.

Since we are considering the two-dimensional problem with

$$\mathbf{u} = (u_x, 0, u_z), \quad \boldsymbol{\phi} = (0, \phi_2, 0), \tag{6}$$

the field equations (1)–(3) reduce to

$$(\lambda + \mu)\frac{\partial}{\partial x}\left(\frac{\partial u_x}{\partial x} + \frac{\partial u_z}{\partial z}\right) + (\mu + K)\nabla^2 u_x - K\frac{\partial \phi_2}{\partial z} - \nu\left(1 + t_1\frac{\partial}{\partial t}\right)\frac{\partial T}{\partial x} = \rho\frac{\partial^2 u_x}{\partial t^2}, \tag{7}$$

$$(\lambda + \mu)\frac{\partial}{\partial z}\left(\frac{\partial u_x}{\partial x} + \frac{\partial u_z}{\partial z}\right) + (\mu + K)\nabla^2 u_z + K\frac{\partial \phi_2}{\partial x} - \nu\left(1 + t_1\frac{\partial}{\partial t}\right)\frac{\partial T}{\partial z} = \rho\frac{\partial^2 u_z}{\partial t^2}, \tag{8}$$

$$\gamma\nabla^2\phi_2 + K\left(\frac{\partial u_x}{\partial z} - \frac{\partial u_z}{\partial x}\right) - 2K\phi_2 = \rho j\frac{\partial^2 \phi_2}{\partial t^2} \quad \text{and} \tag{9}$$

$$K^*\nabla^2 T = \rho C^*\left(\frac{\partial T}{\partial t} + t_0\frac{\partial^2 T}{\partial t^2}\right) + \nu T_0\left(\frac{\partial}{\partial t} + \Xi t_0\frac{\partial^2}{\partial t^2}\right)\left(\frac{\partial u_x}{\partial x} + \frac{\partial u_z}{\partial z}\right). \tag{10}$$

We define the non-dimensional quantities as

$$x' = \frac{\omega^*}{c_1}x, \quad z' = \frac{\omega^*}{c_1}z, \quad t' = \omega^* t, \quad t_1' = \omega^* t_1, \quad t_0' = \omega^* t_0, \quad u_x' = \frac{\rho\omega^* c_1}{\nu T_0}u_x,$$

$$u_z' = \frac{\rho\omega^* c_1}{\nu T_0}u_z, \quad \phi_2' = \frac{\rho c_1^2}{\nu T_0}\phi_2, \quad t_{ij}' = \frac{t_{ij}}{\nu T_0}, \quad m_{ij}' = \frac{\omega^*}{c_1\nu T_0}m_{ij}, \quad T' = \frac{T}{T_0}, \tag{11}$$

where

$$\omega^* = \frac{\rho C^* c_1^2}{K^*}, \quad c_1^2 = (\lambda + 2\mu + K)/\rho.$$

Using equation (11) in equations (7)–(10), we obtain the equations in non-dimensional form, after supressing the primes as

$$\frac{(\lambda + \mu)}{\rho c_1^2}\left(\frac{\partial^2 u_x}{\partial x^2} + \frac{\partial^2 u_z}{\partial x\,\partial z}\right) + \frac{(\mu + K)}{\rho c_1^2}\nabla^2 u_x - \frac{K}{\rho c_1^2}\frac{\partial \phi_2}{\partial z} - \left(1 + t_1\frac{\partial}{\partial t}\right)\frac{\partial T}{\partial x} = \frac{\partial^2 u_x}{\partial t^2}, \tag{12}$$

$$\frac{(\lambda + \mu)}{\rho c_1^2}\left(\frac{\partial^2 u_x}{\partial x\,\partial z} + \frac{\partial^2 u_z}{\partial z^2}\right) + \frac{(\mu + K)}{\rho c_1^2}\nabla^2 u_z + \frac{K}{\rho c_1^2}\frac{\partial \phi_2}{\partial x} - \left(1 + t_1\frac{\partial}{\partial t}\right)\frac{\partial T}{\partial z} = \frac{\partial^2 u_z}{\partial t^2}, \tag{13}$$

$$\nabla^2\phi_2 + \left(\frac{Kc_1^2}{\gamma\omega^{*2}}\right)\left(\frac{\partial u_x}{\partial z} - \frac{\partial u_z}{\partial x}\right) - 2\left(\frac{Kc_1^2}{\gamma\omega^{*2}}\right)\phi_2 = \left(\frac{\rho j c_1^2}{\gamma}\right)\frac{\partial^2 \phi_2}{\partial t^2}, \tag{14}$$

$$\nabla^2 T - \left(\frac{\partial T}{\partial t} + t_0\frac{\partial^2 T}{\partial t^2}\right) = \frac{\nu^2 T_0}{\rho K^*\omega^*}\left[\frac{\partial}{\partial t} + \Xi t_0\frac{\partial^2}{\partial t^2}\right]\left[\frac{\partial u_x}{\partial x} + \frac{\partial u_z}{\partial z}\right]. \tag{15}$$

The displacement components can be written as

$$u_x = \frac{\partial q}{\partial x} + \frac{\partial \psi}{\partial z}, \quad u_z = \frac{\partial q}{\partial z} - \frac{\partial \psi}{\partial x}, \quad \text{and} \quad \psi = (-\mathbf{U})_y, \tag{16}$$

where $q(x, z, t)$ and $\psi(x, z, t)$ are scalar potential functions and $\mathbf{U}(x, z, t)$ is the vector potential function.
Using equation (16) in equations (12)–(15), we obtain

$$\left(\nabla^2 - \frac{\partial^2}{\partial t^2}\right) q - \left(1 + t_1 \frac{\partial}{\partial t}\right) T = 0, \tag{17}$$

$$\left(\nabla^2 - a_3 \frac{\partial^2}{\partial t^2}\right) \psi - a_4 \phi_2 = 0 \tag{18}$$

$$\left[\nabla^2 - 2a_1 - a_2 \frac{\partial^2}{\partial t^2}\right] \phi_2 + a_1 \nabla^2 \psi = 0, \tag{19}$$

$$\left(\nabla^2 - \frac{\partial}{\partial t} - t_0 \frac{\partial^2}{\partial t^2}\right) T - \varepsilon \left(\frac{\partial}{\partial t} + \Xi t_0 \frac{\partial^2}{\partial t^2}\right) \nabla^2 q = 0, \tag{20}$$

where

$$a_1 = \frac{K c_1^2}{\gamma \omega^{*2}}, \quad a_2 = \frac{\rho j c_1^2}{\gamma}, \quad a_3 = \frac{\rho c_1^2}{\mu + K}, \quad a_4 = \frac{K}{\mu + K}$$

and

$$\varepsilon = (v^2 T_0 / \rho K^* \omega^*). \tag{21}$$

Applying the Laplace and Fourier transforms defined by

$$\bar{f}(p) = \int_0^\infty \mathrm{e}^{-pt} f(t)\, \mathrm{d}t \quad \text{and} \quad \hat{f}(\xi, z, p) = \int_{-\infty}^{\infty} \bar{f}(x, z, p)\, \mathrm{e}^{\mathrm{i}\xi x}\, \mathrm{d}x \tag{22}$$

on equations (17)–(20) and then eliminating $\hat{T}$ and $\hat{\phi}_2$ from the resulting expressions, we obtain

$$\left[\frac{\mathrm{d}^4}{\mathrm{d}z^4} + A \frac{\mathrm{d}^2}{\mathrm{d}z^2} + D\right] [\hat{q}] = 0 \tag{23}$$

and

$$\left[\frac{\mathrm{d}^4}{\mathrm{d}z^4} + B \frac{\mathrm{d}^2}{\mathrm{d}z^2} + E\right] [\hat{\psi}] = 0, \tag{24}$$

where

$$\begin{aligned}
A &= -[2\xi^2 + p^2 + p(1 + t_0 p) + \varepsilon p(1 + t_1 p)(1 + t_0 p \Xi)], \\
D &= \xi^4 + \xi^2 [p^2 + p(1 + t_0 p) + \varepsilon p(1 + t_1 p)(1 + t_0 p \Xi)] + p^3 (1 + t_0 p), \\
B &= -[2\xi^2 + 2a_1 + p^2 (a_2 + a_3) - a_1 a_4], \\
E &= \xi^4 + \xi^2 [2a_1 + p^2 (a_2 + a_3) - a_1 a_4] + a_3 p^2 (2a_1 + a_2 p^2).
\end{aligned} \tag{25}$$

The solutions of equations (23) and (24) are

$$\hat{q} = A_1 \exp(-\xi_1 z) + A_2 \exp(-\xi_2 z), \tag{26}$$

$$\hat{T} = Q_1 A_1 \exp(-\xi_1 z) + Q_2 A_2 \exp(-\xi_2 z), \tag{27}$$

$$\hat{\psi} = A_3 \exp(-\xi_3 z) + A_4 \exp(-\xi_4 z), \tag{28}$$

$$\hat{\phi}_2 = Q_3 A_3 \exp(-\xi_3 z) + Q_4 A_4 \exp(-\xi_4 z), \tag{29}$$

where $\xi_{1,2}^2$ and $\xi_{3,4}^2$ are roots of equations (23) and (24), respectively, and are given by

$$\xi_{1,2}^2 = [-A \pm \sqrt{A^2 - 4D}]/2, \quad \xi_{3,4}^2 = [-B \pm \sqrt{B^2 - 4E}]/2 \tag{30}$$

and

$$Q_{1,2} = \frac{1}{(1 + t_1 p)} [\xi_{1,2}^2 - \xi^2 - p^2], \quad Q_{3,4} = \frac{1}{a_4} [\xi_{3,4}^2 - \xi^2 - a_3 p^2]. \tag{31}$$

2.1. CASE I: MECHANICAL SOURCE ACTING ON THE SURFACE

Plane boundary is subjected to an instantaneous normal point force and the boundary surface is isothermal. Therefore, the boundary conditions in this case are

$$t_{zz} = -P\delta(x)\delta(t), \quad t_{zx} = m_{zy} = T = 0, \quad \text{at } z = 0, \tag{32}$$

where P is the magnitude of the force applied.

Making use of equations (4), (5), (11) and (16) in the boundary conditions (32) and applying the transforms defined by equation (22) and substituting the values of $\hat{q}$, $\hat{T}$, $\hat{\psi}$ and $\hat{\phi}_2$ from equations (26)–(29) in the resulting expressions, we obtain the expressions for displacement components, stresses and temperature field as

$$\hat{u}_x = -\frac{1}{\Delta} [\mathrm{i}\xi(\Delta_1 \mathrm{e}^{-\xi_1 z} + \Delta_2 \mathrm{e}^{-\xi_2 z}) + \xi_3 \Delta_3 \mathrm{e}^{-\xi_3 z} + \xi_4 \Delta_4 \mathrm{e}^{-\xi_4 z}], \tag{33}$$

$$\hat{u}_z = -\frac{1}{\Delta} [\xi_1 \Delta_1 \mathrm{e}^{-\xi_1 z} + \xi_2 \Delta_2 \mathrm{e}^{-\xi_2 z} - \mathrm{i}\xi(\Delta_3 \mathrm{e}^{-\xi_3 z} + \Delta_4 \mathrm{e}^{-\xi_4 z})], \tag{34}$$

$$\hat{t}_{zz} = \frac{1}{\Delta} [f_1 \Delta_1 \mathrm{e}^{-\xi_1 z} + f_2 \Delta_2 \mathrm{e}^{-\xi_2 z} - \mathrm{i}b_2 \xi(\xi_3 \Delta_3 \mathrm{e}^{-\xi_3 z} + \xi_4 \Delta_4 \mathrm{e}^{-\xi_4 z})], \tag{35}$$

$$\hat{t}_{zx} = \frac{1}{\Delta} [\mathrm{i}\xi b_2(\xi_1 \Delta_1 \mathrm{e}^{-\xi_1 z} + \xi_2 \Delta_2 \mathrm{e}^{-\xi_2 z}) + f_3 \Delta_3 \mathrm{e}^{-\xi_3 z} + f_4 \Delta_4 \mathrm{e}^{-\xi_4 z}], \tag{36}$$

$$\hat{m}_{zy} = \frac{-b_6}{\Delta} [Q_3 \xi_3 \Delta_3 \mathrm{e}^{-\xi_3 z} + Q_4 \xi_4 \Delta_4 \mathrm{e}^{-\xi_4 z}], \tag{37}$$

$$\hat{T} = \frac{1}{\Delta} [Q_1 \Delta_1 \mathrm{e}^{-\xi_1 z} + Q_2 \Delta_2 \mathrm{e}^{-\xi_2 z}], \tag{38}$$

where

$$\Delta = Q_1\xi_3 Q_3(f_2 f_4 - b_2^2\xi^2\xi_2\xi_4) - Q_1\xi_4 Q_4(f_2 f_3 - b_2^2\xi^2\xi_2\xi_3)$$
$$- Q_2\xi_3 Q_3(f_1 f_4 - b_2^2\xi^2\xi_1\xi_4) + Q_2\xi_4 Q_4(f_1 f_3 - b_2^2\xi^2\xi_1\xi_3),$$
$$\Delta_1 = PQ_2(f_4\xi_3 Q_3 - f_3\xi_4 Q_4), \quad \Delta_2 = PQ_1(f_3\xi_4 Q_4 - f_4\xi_3 Q_3),$$
$$\Delta_3 = P\xi_4 Q_4 b_2\xi(\xi_2 Q_1 - \xi_1 Q_2), \quad \Delta_4 = P\xi_3 Q_3 b_2\xi(\xi_1 Q_2 - \xi_2 Q_1),$$
$$f_i = \xi_i^2 - b_1\xi^2 - (1 + t_1 p)Q_i \quad (i = 1, 2)$$
$$f_j = b_3\xi_j^2 + b_4\xi^2 - b_5 Q_j \quad (j = 3, 4)$$

$$b_1 = \frac{\lambda}{\rho c_1^2}, \quad b_2 = \frac{2\mu + K}{\rho c_1^2}, \quad b_3 = b_4 + b_5, \quad b_4 = \frac{\mu}{\rho c_1^2}, \quad b_5 = \frac{K}{\rho c_1^2}, \quad b_6 = \frac{\omega^{*2}\gamma}{\rho c_1^4}. \tag{39}$$

Subcase I: For L–S theory, A and D in the expressions (33)–(38), take the form

$$A = -[2\xi^2 + p^2 + p(1 + t_0 p) + \varepsilon p(1 + t_0 p)],$$
$$D = \xi^4 + \xi^2[p^2 + p(1 + t_0 p) + \varepsilon p(1 + t_0 p)] + p^3(1 + t_0 p)$$

and

$$Q_i = (\xi_i^2 - \xi^2 - p^2), \quad (i = 1, 2). \tag{40}$$

Subcase II: For G–L theory, A and D in the expressions (33)–(38), become

$$A = -[2\xi^2 + p^2 + p(1 + t_0 p) + \varepsilon p(1 + t_1 p)],$$
$$D = \xi^4 + \xi^2[p^2 + p(1 + t_0 p) + \varepsilon p(1 + t_1 p)] + p^3(1 + t_0 p). \tag{41}$$

Subcase III: For the Green and Naghdi theory [8], equations (1), (3) and (4) are written as

$$(\lambda + \mu)\nabla(\nabla\cdot\mathbf{u}) + (\mu + K)\nabla^2\mathbf{u} + K\nabla x\boldsymbol{\phi} - \nu\nabla T = \frac{\rho\partial^2\mathbf{u}}{\partial t^2}, \tag{42}$$

$$K^*\nabla^2 T = \rho C^*\frac{\partial^2 T}{\partial t^2} + \nu T_0\frac{\partial^2(\nabla\cdot\mathbf{u})}{\partial t^2}, \tag{43}$$

$$t_{ij} = \lambda u_{r,r}\delta_{ij} + \mu(u_{i,j} + u_{j,i}) + K(u_{j,i} - \varepsilon_{ijr}\phi_r) - \nu T\delta_{ij} \tag{44}$$

and K^* is not the usual thermal conductivity but a material characteristic constant of the theory and in the G–N theory is given by $K^*(= C^*(\lambda + 2\mu)/4)$.

With these considerations, A, D and f_i $(i = 1, 2)$ now take the form

$$A = -[2\xi^2 + p^2 + p^2(1 + \varepsilon)], \quad D = \xi^4 + p^4 + \xi^2 p^2(2 + \varepsilon)$$

and

$$f_i = \xi_i^2 - b_1\xi^2 - Q_i, \quad i = 1, 2. \tag{45}$$

2.2. CASE II: THERMAL POINT SOURCE ACTING ON THE SURFACE

When the plane boundary is stress free and subjected to an instantaneous thermal point source, the boundary conditions in this case are

$$t_{zz} = t_{zx} = m_{zy} = 0, \quad T = P\delta(x)\delta(t), \quad \text{at } z = 0, \tag{46}$$

where P is the magnitude of the constant temperature applied on the boundary.

With the help of these boundary conditions (46), the expressions for displacement components, force stresses, couple stress and temperature field are obtained with Δ_i replaced by Δ_i' $(i = 1, \ldots, 4)$, where

$$\begin{aligned}
\Delta_1' &= P[\xi_3 Q_3(f_2 f_4 - b_2^2 \xi^2 \xi_2 \xi_4) - \xi_4 Q_4(f_2 f_3 - b_2^2 \xi^2 \xi_2 \xi_3)], \\
\Delta_2' &= P[\xi_4 Q_4(f_1 f_3 - b_2^2 \xi^2 \xi_1 \xi_3) - \xi_3 Q_3(f_1 f_4 - b_2^2 \xi^2 \xi_1 \xi_4)], \\
\Delta_3' &= P\xi_4 Q_4 b_2 \xi(f_1 \xi_2 - f_2 \xi_1), \quad \Delta_4' = P\xi_3 Q_3 b_2 \xi(f_2 \xi_1 - f_1 \xi_2),
\end{aligned} \tag{47}$$

Particular cases:

Replacing Δ_i by Δ_i' $(i = 1, \ldots, 4)$ defined by equation (47) in the expressions (33)–(38), we obtain the displacement components, stresses and temperature distribution as

(i) For L–S theory with A, D and Q_i $(i = 1, 2)$ defined by equation (40).
(ii) For G–L theory with A and D given by equation (41).
(iii) For G–N theory with A, D and f_i $(i = 1, 2)$ given by equation (45).

3. INVERSION OF THE TRANSFORMS

To obtain the solution of the problem in the physical domain, we must invert the transforms in equations (33)–(38) for all the theories in case of mechanical source and thermal source applied. These expressions are functions of z, the parameters of Laplace and Fourier transforms p and ξ, respectively, and hence are of the form $\hat{f}(\xi, z, p)$. To get the function $f(x, z, t)$ in the physical domain, first we invert the Fourier transform using

$$\bar{f}(x, z, p) = \int_{-\infty}^{\infty} \mathrm{e}^{-\mathrm{i}\xi x} \hat{f}(\xi, z, p)\, \mathrm{d}\xi = 2 \int_0^{\infty} (\cos(\xi x) f_e - \mathrm{i} \sin(\xi x) f_o)\, \mathrm{d}\xi, \tag{48}$$

where f_e and f_o are even and odd parts of the function $\hat{f}(\xi, z, p)$, respectively. Thus, expression (48) gives us the Laplace transform $\bar{f}(x, z, p)$ of the function $f(x, z, t)$.

Now, for the fixed values of ξ, x and z, the function $\bar{f}(x, z, p)$ in the expression (48) can be considered as the Laplace transform $\bar{g}(p)$ of same function $g(t)$. Following Honig and Hirdes [16], the Laplace transformed function $\bar{g}(p)$ can be inverted as follows:

The function $g(t)$ can be obtained by using

$$g(t) = \frac{1}{2\pi \mathrm{i}} \int_{C - \mathrm{i}\infty}^{C + \mathrm{i}\infty} \mathrm{e}^{\mathrm{pt}} \bar{g}(p)\, \mathrm{d}p, \tag{49}$$

where C is an arbitrary real number greater than all the real parts of the singularities of $\bar{g}(p)$. Taking $p = C + \mathrm{i}y$, we get

$$g(t) = \frac{\mathrm{e}^{Ct}}{2\pi} \int_{-\infty}^{\infty} \mathrm{e}^{\mathrm{i}ty} \bar{g}(C + \mathrm{i}y)\, \mathrm{d}y. \tag{50}$$

Now, taking $e^{-Ct}g(t)$ as $h(t)$ and expanding it as Fourier series in $[0, 2L]$, we obtain approximately the formula

$$g(t) = g_\infty(t) + E_D \tag{51}$$

where

$$g_\infty(t) = \frac{C_0}{2} + \sum_{k=1}^{\infty} C_k, \quad 0 \leqslant t \leqslant 2L, \tag{52}$$

and

$$C_k = \frac{e^{Ct}}{L} \operatorname{Re}\left[e^{ik\pi t/L}\, \bar{g}\left(C + \frac{ik\pi}{L}\right)\right],$$

where E_D is the discretization error and can be made arbitrarily small by choosing C large enough.

Since the infinite series in equation (52) can be summed up only to a finite number of N terms, so the approximate value of $g(t)$ becomes

$$g_N(t) = \frac{C_0}{2} + \sum_{k=1}^{N} C_k \quad \text{for } 0 \leqslant t \leqslant 2L. \tag{53}$$

Now, we introduce a truncation error E_T that must be added to the discretization error to produce the total approximate error in evaluating $g(t)$ using the above formula. The discretization error is reduced by using the "Korrecktur method" and then the "ε-algorithm" is used to reduce the truncation error and hence to accelerate the convergence.

The Korrecktur method formula, to evaluate the function $g(t)$ is

$$g(t) = g_\infty(t) - e^{-2CL}\, g_\infty(2L + t) + E'_D,$$

where $|E'_D| \ll |E_D|$.

Thus, the approximate value of $g(t)$ becomes

$$g_{N_k}(t) = g_N(t) - e^{-2CL}\, g_{N'}(2L + t), \tag{54}$$

where N' is an integer such than $N' < N$.

We shall now describe the ε-algorithm, which is used to accelerate the convergence of the series in equation (53). Let N be an odd natural number and $s_m = \sum_{k=1}^{m} C_k$ be the sequence of partial sums of equation (53). We define the ε-sequence by

$$\varepsilon_{0,m} = 0, \quad \varepsilon_{1,m} = s_m,$$

$$\varepsilon_{n+1,m} = \varepsilon_{n-1,m+1} + \frac{1}{\varepsilon_{n,m+1} - \varepsilon_{n,m}}, \quad n, m = 1, 2, 3, \ldots.$$

The sequence $\varepsilon_{1,1}, \varepsilon_{3,1}, \ldots, \varepsilon_{N,1}$ converges to $g(t) + E_D - C_0/2$ faster than the sequence of partial sums s_m, $m = 1, 2, 3, \ldots$. The actual procedure to invert the Laplace transform consists of equation (54) together with the ε-algorithm. The values of C and L are choosen according to the criteria outlined by Honig and Hirdes [16].

The last step is to calculate the integral in equation (48). The method for evaluating this integral is described by Press *et al.* [17], which involves the use of Romberg's integration

with adaptive step size. This, also uses the results from successive refinements of the extended trapezoidal rule followed by extrapolation of the results to the limit when the step size tends to zero.

4. NUMERICAL RESULTS AND DISCUSSION

We take the case of magnesium crystal [18] like material subjected to mechanical and thermal disturbance for numerical calculations. The physical constants used are: $\rho = 1{\cdot}74\ \text{g/cm}^3$, $j = 0{\cdot}2 \times 10^{-15}\ \text{cm}^2$, $\lambda = 9{\cdot}4 \times 10^{11}\ \text{dyn/cm}^2$, $\mu = 4{\cdot}0 \times 10^{11}\ \text{dyn/cm}^2$. $K = 1{\cdot}0 \times 10^{11}\ \text{dyn/cm}^2$, $\gamma = 0{\cdot}779 \times 10^{-4}\ \text{dyn}$, $K^* = 0{\cdot}6 \times 10^{-2}\ \text{cal/cm s}^\circ\text{C}$, $C^* = 0{\cdot}23\ \text{cal/g}^\circ\text{C}$, $\varepsilon = 0{\cdot}073$, $P = 1$, $T_0 = 23^\circ\text{C}$, $t_0 = 6{\cdot}131 \times 10^{-13}\ \text{s}$, $t_1 = 8{\cdot}765 \times 10^{-13}\ \text{s}$.

The distribution of normal displacement, normal force stress, tangential couple stress and temperature field with distance 'x' at the plane $z = 1$ for Lord–Shulman (L–S) theory, Green-Lindsay (G–L) theory and Green Naghdi (G–N) theory have been shown by solid line (—), small dashed line (- - - -) and long dashed line (– –) respectively. These distributions are shown graphically in Figures 1–24 at three different times, 0·1, 0·5 and 1·5 s for mechanical and thermal sources.

4.1. CASE I: MECHANICAL SOURCE

Variations of t_{zz} at $t = 0{\cdot}1$ s for the three theories (L–S, G–L and G–N) have been shown in Figure 1 and it is observed that the behaviour of t_{zz} for G–L theory is opposite to L–S and G–N theories. The values of u_z and m_{zy} decrease sharply as x lies between $0 \leqslant x \leqslant 2{\cdot}0$ and oscillate as x increases further for L–S, G–L and G–N theories at $t = 0{\cdot}01$ s and these variations have been shown in Figures 2 and 3 respectively. Figure 4 shows the variations of temperature field T at $t = 0{\cdot}1$ s and it is observed that the range of variations of temperature field for L–S and G–L theories is very small in comparison to G–N theory.

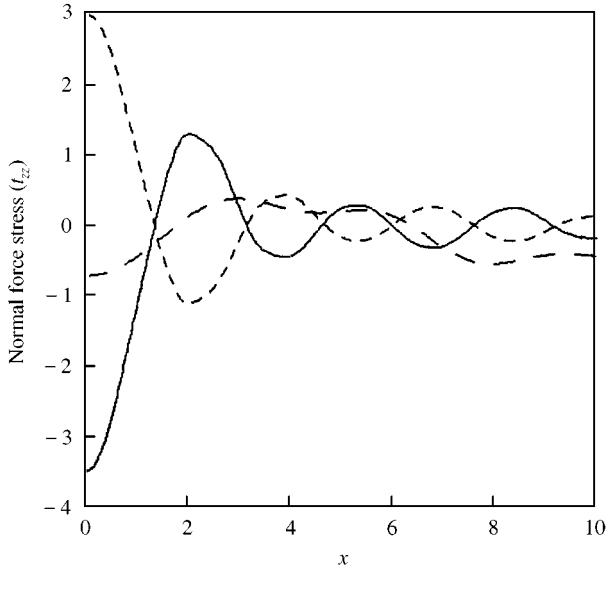

Figure 1. Variations of normal force stress t_{zz} with distance x at $t = 0{\cdot}1$ s (mechanical source). ——, L–S; - - - -, G–L; — —, G–N.

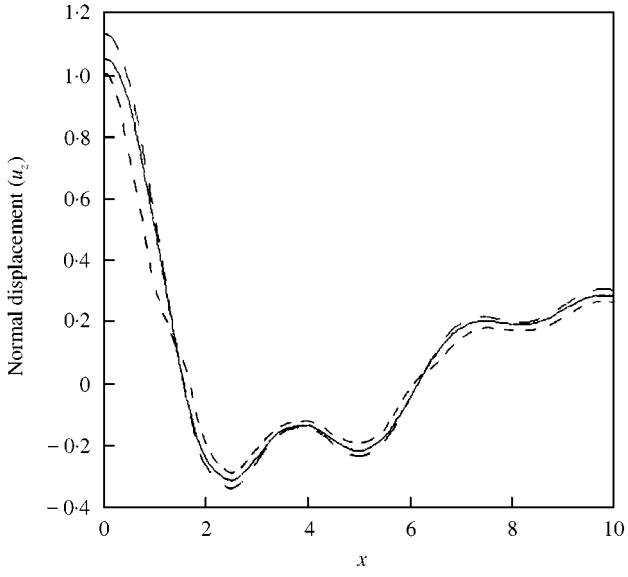

Figure 2. Variations of normal displacement u_z with distance x at $t = 0{\cdot}1$ s (mechanical source). ——, L–S; – – – –, G–L; — —, G–N.

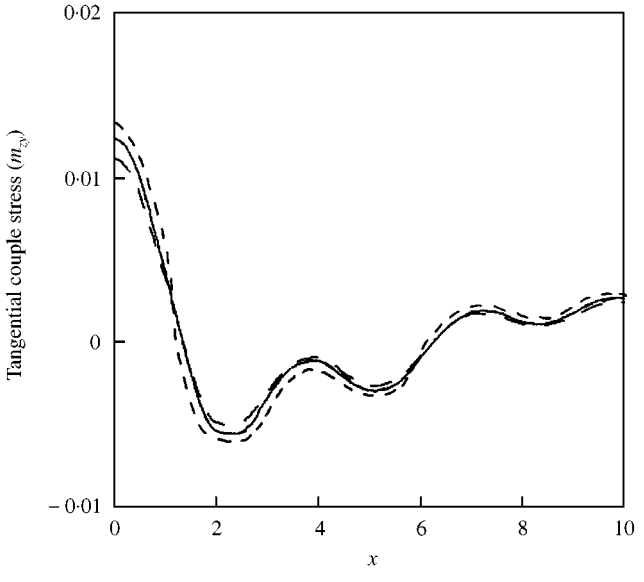

Figure 3. Variations of tangential couple stress m_{zy} with distance x at $t = 0{\cdot}1$ s (mechanical source). ——, L–S; – – – –, G–L; — —, G–N.

Figure 5 depicts the variations of t_{zz} at $t = 0{\cdot}5$ s and it is noticed that the variations for L–S and G–N theories are oscillatory and lie in a very small range in comparison to G–L theory. The behaviour of u_z and m_{zy} for three different theories is similar although their magnitude values are different as x varies from 0 to 10 at $t = 0{\cdot}5$ s and these variations are shown in Figures 6 and 7 respectively. Figure 8 shows the variations of temperature field

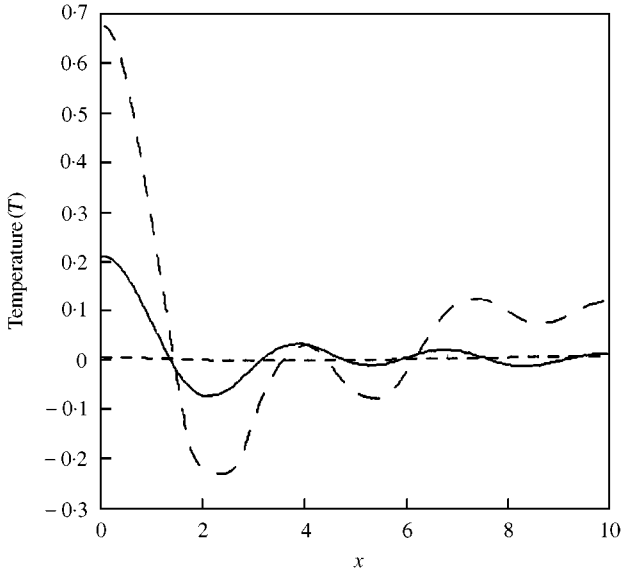

Figure 4. Variations of temperature field T with distance x at $t = 0{\cdot}1$ s (mechanical source). ——, L–S; – – – –, G–L; ——, G–N.

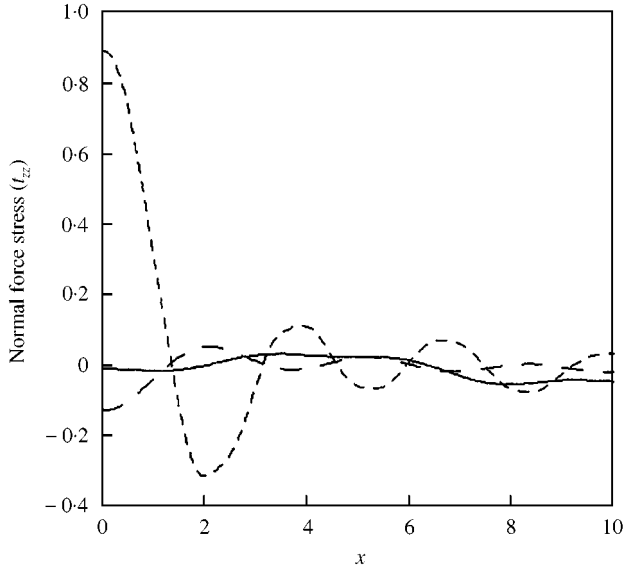

Figure 5. Variations of normal force stress t_{zz} with distance x at $t = 0{\cdot}5$ s (mechanical source). ——, L–S; – – – –, G–L; ——, G–N.

T at $t = 0{\cdot}5$ s and it is noticed that for G–L theory variations take place in a very small range in comparison to L–S and G–N theories.

Variations of t_{zz} at $t = 1{\cdot}5$ s for L–S and G–L theories lie in a large range and have opposite behaviour as compared to G–N theory and these variations have been shown in Figure 9. It is further noticed that for L–S and G–L theories, there is a sharp increase in the values of t_{zz}, whereas the values decrease for G–N theory as x lies between $0 \leqslant x \leqslant 2{\cdot}0$. As

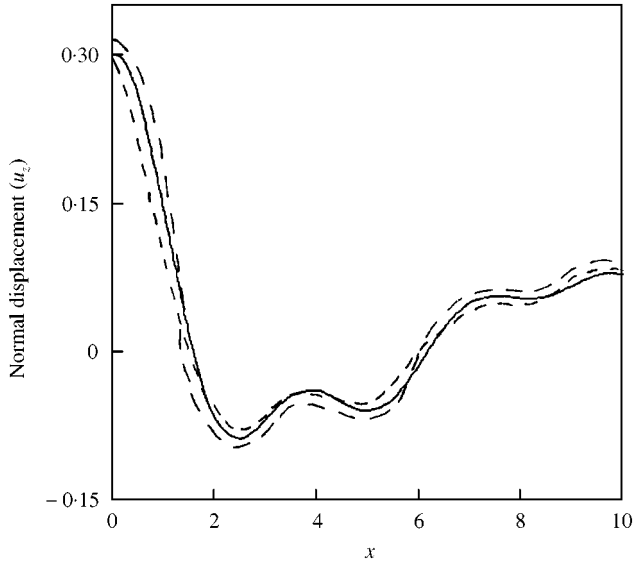

Figure 6. Variations of normal displacement u_z with distance x at $t = 0{\cdot}5$ s (mechanical source). ——, L–S; – – – –, G–L; ——, G–N.

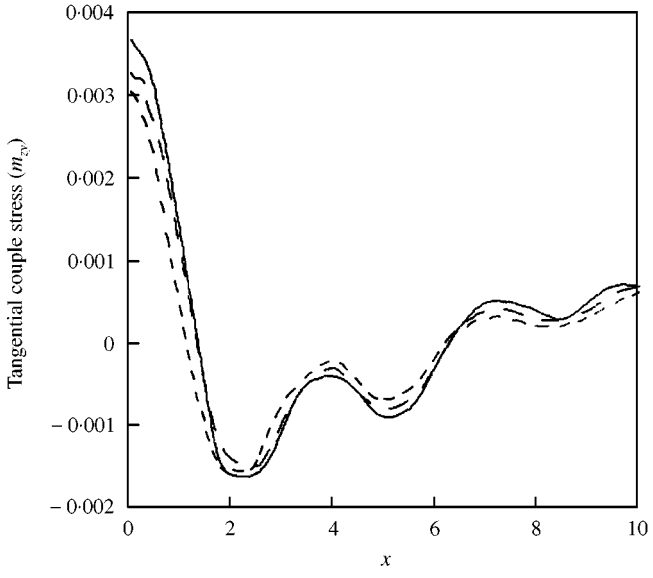

Figure 7. Variations of tangential couple stress m_{zy} with distance x at $t = 0{\cdot}5$ s (mechanical source). ——, L–S; – – – –, G–L; ——, G–N.

x increases further, the values of t_{zz} oscillate for all the three theories. Figure 10 shows the variations of u_z at $t = 1{\cdot}5$ s and it is observed that the behaviour of u_z is similar for all the three different theories although its magnitude values are different. The variations of m_{zy} are oscillatory for all the three theories at $t = 1{\cdot}5$ s and values of m_{zy} lie in a very small range as depicted in Figure 11. Figure 12 shows the behaviour of temperature field T at $t = 1{\cdot}5$ s. It is noticed that the variations for G–L theory lie in a very small range as compared to L–S and

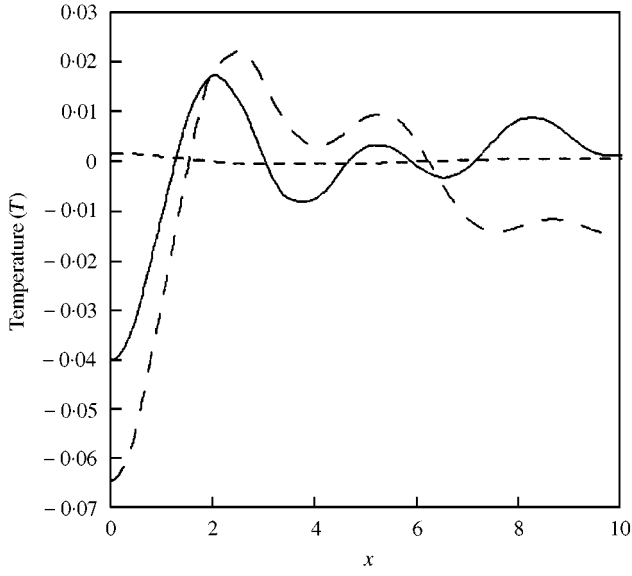

Figure 8. Variations of temperature field T with distance x at $t = 0{\cdot}5$ s (mechanical source). ——, L–S; – – – –, G–L; — —, G–N.

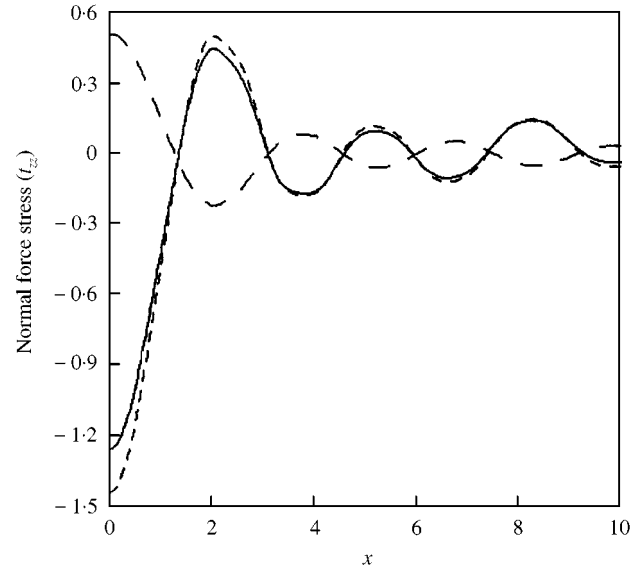

Figure 9. Variations of normal force stress t_{zz} with distance x at $t = 1{\cdot}5$ s (mechanical source). ——, L–S; – – – –, G–L; — —, G–N.

G–N theories, although the variations for L–S theory are in an opposite manner to G–N theory.

4.2. CASE II: THERMAL SOURCE

The variations of t_{zz} at $t = 0{\cdot}1$ s are shown in Figure 13, where, the original values for G–L theory have been divided by 10^3 to depict the comparison simultaneously with L–S

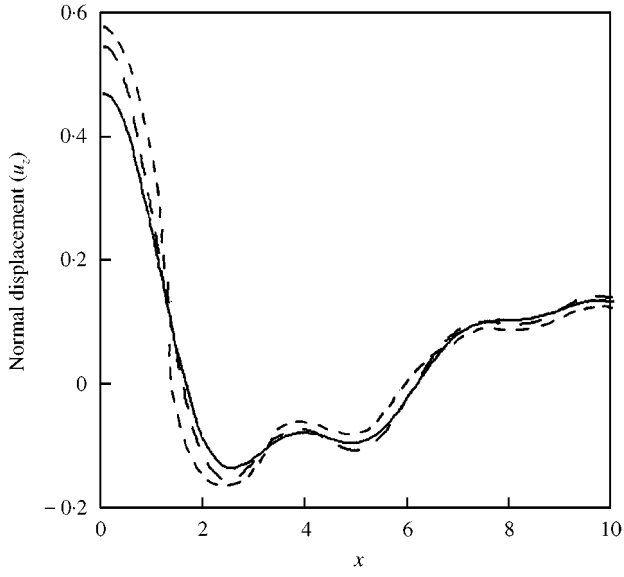

Figure 10. Variations of normal displacement u_z with distance x at $t = 1{\cdot}5$ s (mechanical source). ——, L–S; – – – –, G–L; — —, G–N.

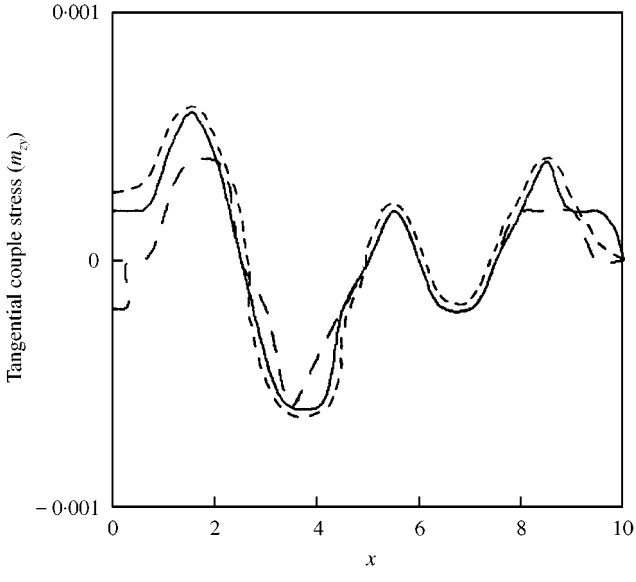

Figure 11. Variations of tangential couple stress m_{zy} with distance x at $t = 1{\cdot}5$ s (mechanical source). ——, L–S; – – – –, G–L; — —, G–N.

and G–N theories and it is observed that the values for L–S theory lie in a very small range in comparison to G–L and G–N theories. The variations of u_z at $t = 0{\cdot}1$ s are shown in Figure 14. The values of u_z for L–S theory vary in a very short range in comparison to G–L and G–N theories and the variations for G–L theory have been shown after dividing the original values by 10^2. Also, the behaviour of u_z for G–N theory is opposite from those for L–S and G–L theories. Variations of m_{zy} at $t = 0{\cdot}1$ s are almost similar for three different

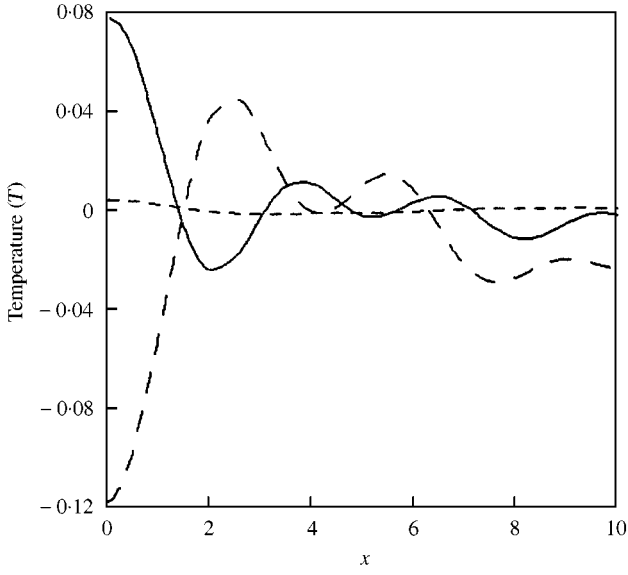

Figure 12. Variations of temperature field T with distance x at $t = 1{\cdot}5$ s (mechanical source). ——, L–S; – – – –, G–L; — —, G–N.

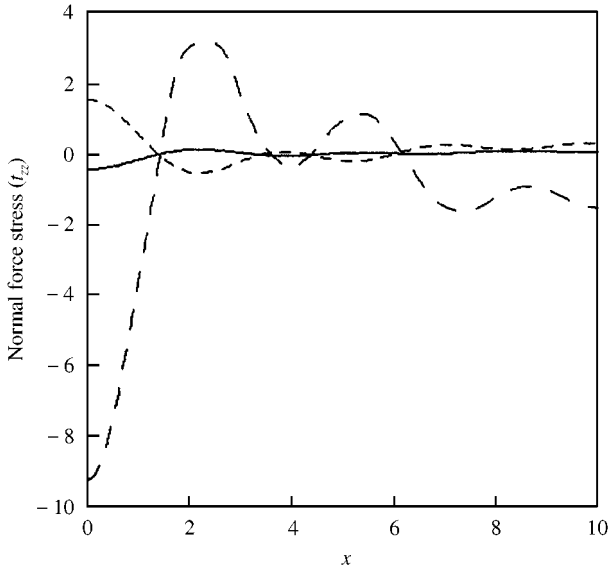

Figure 13. Variations of normal force stress t_{zz} with distance x at $t = 0{\cdot}1$ s (thermal source). ——, L–S; – – – –, G–L; — —, G–N.

theories although the magnitude values are different as shown in Figure 15, where the original values of m_{zy} for G–L theory have been divided by 10 to depict the comparison of three different theories. The variations of temperature field T at $t = 0{\cdot}1$ s are shown in Figure 16, and it is observed that the behaviour of T for the three different theories is different.

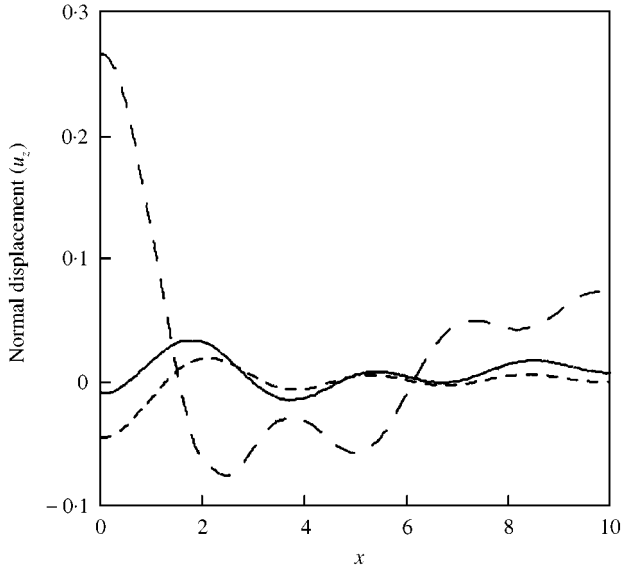

Figure 14. Variations of normal displacement u_z with distance x at $t = 0{\cdot}1$ s (thermal source). ——, L–S; – – – –, G–L; — —, G–N.

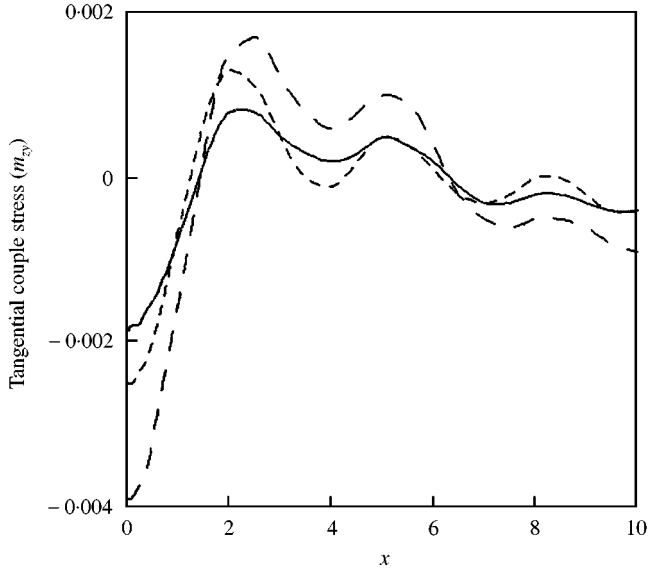

Figure 15. Variations of tangential couple stress m_{zy} with distance x at $t = 0{\cdot}1$ s (thermal source). ——, L–S; – – – –, G–L; — —, G–N.

Figure 17 depicts the variations of t_{zz} at $t = 0{\cdot}5$ s and it is observed that values of t_{zz} for L–S theory lie in a very small range in comparison to G–L and G–N theories and the behaviour of t_{zz} for the three theories is also different. Variations of u_z at $t = 0{\cdot}5$ s are shown in Figure 18, where the original values for L–S theory have been multiplied by 10 and the behaviour of u_z for the three theories is different to each other. From Figure 19, it is

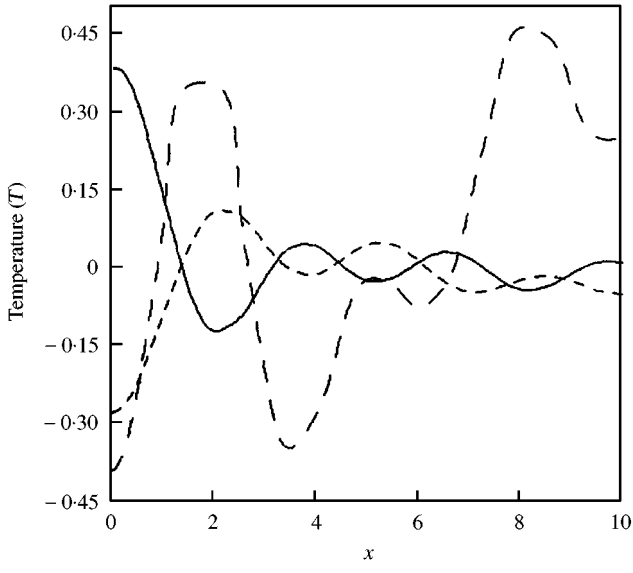

Figure 16. Variations of temperature field T with distance x at $t = 0{\cdot}1$ s (thermal source). ——, L–S; – – – –, G–L; ——, G–N.

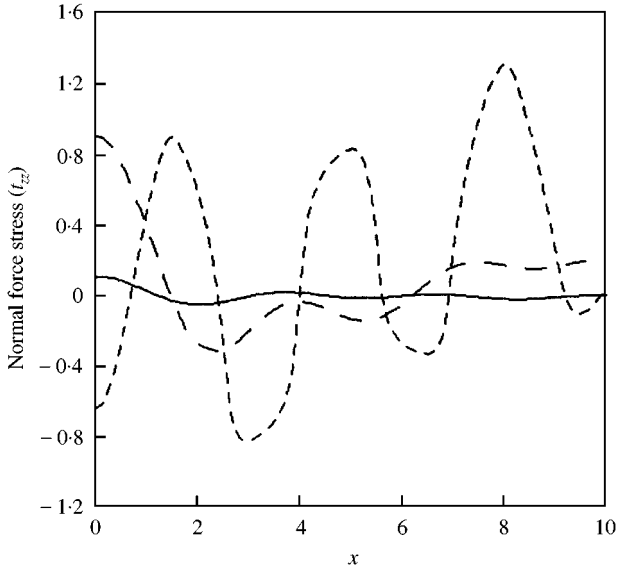

Figure 17. Variations of normal force stress t_{zz} with distance x at $t = 0{\cdot}5$ s (thermal source). ——, L–S; – – – –, G–L; ——, G–N.

observed that variations of m_{zy} for L–S and G–L theories lie in a very small range in comparison to G–N theory at $t = 0{\cdot}5$ s. The range of variations of temperature field for G–L and G–N theories is small in comparison to L–S theory and the variations for the three theories are also different and these variations are shown in Figure 20 at $t = 0{\cdot}5$ s.

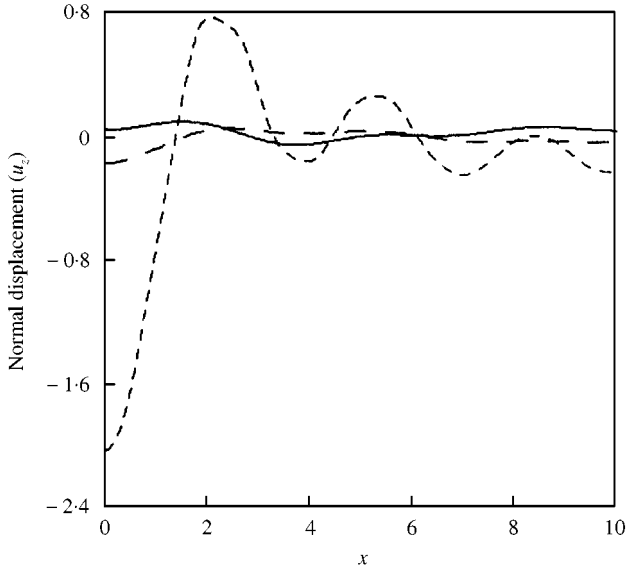

Figure 18. Variations of normal displacement u_z with distance x at $t = 0{\cdot}5$ s (thermal source). ——, L–S; – – – –, G–L; — —, G–N.

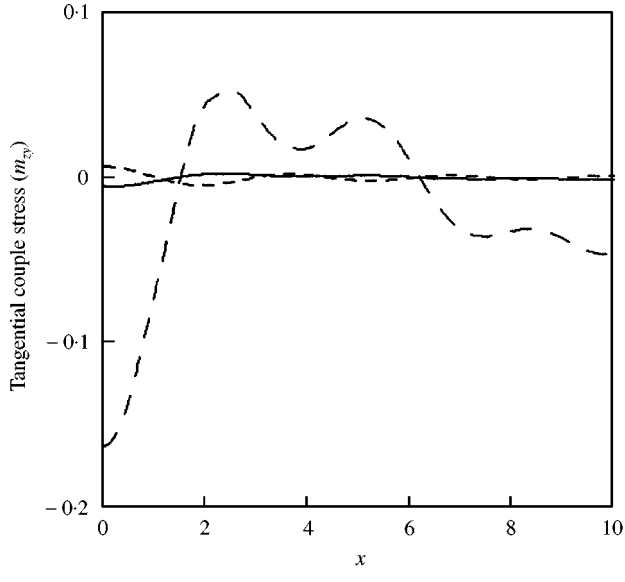

Figure 19. Variations of tangential couple stress m_{zy} with distance x at $t = 0{\cdot}5$ s (thermal source). ——, L–S; – – – –, G–L; — —, G–N.

The values of t_{zz} at $t = 1{\cdot}5$ s for L–S theory lie in a very small range as compared to G–L and G–N theories and the behaviour of t_{zz} for L–S theory is observed to be different from G–L and G–N theories as illustrated in Figure 21. The values of u_z at $t = 1{\cdot}5$ s are again observed to be very small for L–S theory in comparison to G–L and G–N theories in Figure 22, where, the behaviour of u_z for the three theories is different. The behaviour of

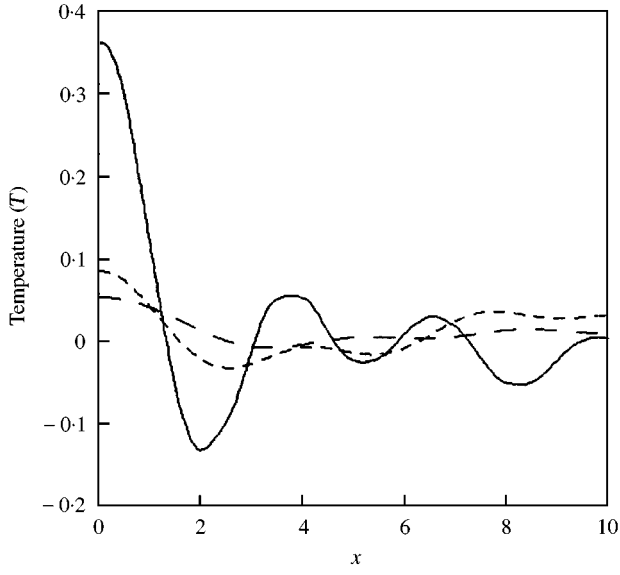

Figure 20. Variations of temperature field T with distance x at $t = 0{\cdot}5$ s (thermal source). ——, L–S; – – – –, G–L; ——, G–N.

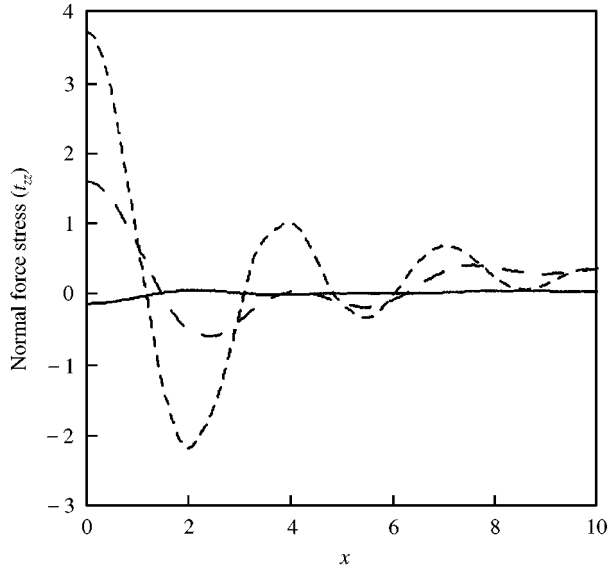

Figure 21. Variations of normal force stress t_{zz} with distance x at $t = 1{\cdot}5$ s (thermal source). ——, L–S; – – – –, G–L; ——, G–N.

m_{zy} for the three different theories is shown in Figure 23 at $t = 1{\cdot}5$ s and it is noticed that the range of variation for G–N theory is very small in comparison to L–S and G–L theories and the behaviour for G–N theory is also different from L–S and G–L theories. The values of temperature field T for L–S and G–L theories lie in a very small range in comparison to G–N theory as shown in Figure 24 at $t = 1{\cdot}5$ s and the behaviour of T for the three theories is also observed to be different.

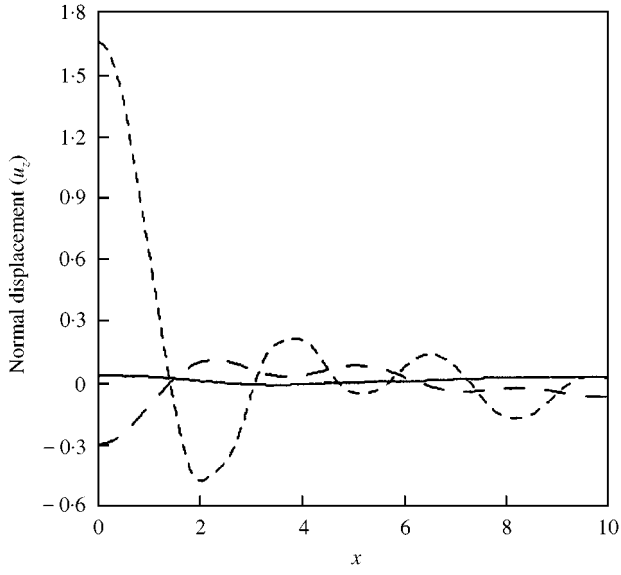

Figure 22. Variations of normal displacement u_z with distance x at $t = 1{\cdot}5$ s (thermal source). ——, L–S; – – – –, G–L; ——, G–N.

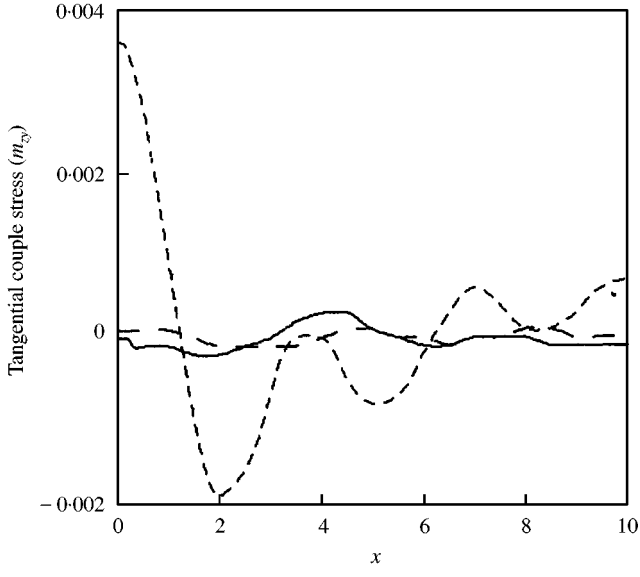

Figure 23. Variations of tangential couple stress m_{zy} with distance x at $t = 1{\cdot}5$ s (thermal source). ——, L–S; – – – –, G–L; ——, G–N.

5. CONCLUSIONS

The magnitude of variations of the normal force stress, normal displacement, tangential couple stress and temperature field is observed to have large values at small times, which then become smaller and smaller with the passage of time. Also, the values of these quantities are observed to be different for the three theories (L–S, G–L and G–N) for both

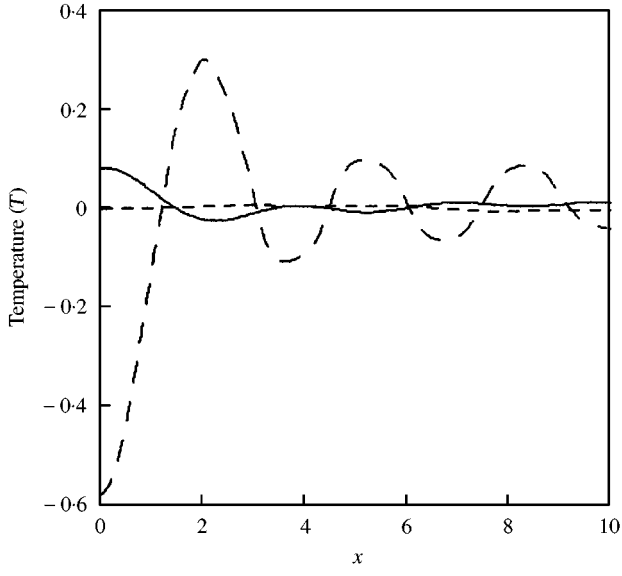

Figure 24. Variations of temperature field T with distance x at $t = 1{\cdot}5$ s (thermal source). ——, L–S; – – – –, G–L; ——, G–N.

the cases and at all the three times. Since, the source applied in both the cases (mechanical and thermal source) is instantaneous, so the range of distribution for all the expressions becomes small with the increase in value of distance 'x'. The resulting stresses and displacements can be used in estimating the effects of a surface pressure wave.

REFERENCES

1. A. C. ERINGEN 1966 *Journal of Mathematical Mechanics* **15**, 909–923. Linear theory of Micropolar elasticity.
2. A. C. ERINGEN 1966 *Journal of Mathematical Mechanics* **16**, 1–18. Theory of micropolar fluids.
3. A. C. ERINGEN 1976 A. C. Eringen editor, Continuum Physics. Vol. IV, 205–267. New York: Academic Press, Non-local polar field theories.
4. H. W. LORD and Y. SHULMAN 1967 *Journal of the Mechanics and Physics of Solids* **15**, 299–306. A generalized dynamical theory of thermoelasticity.
5. A. E. GREEN and K. A. LINDSAY 1972 *Journal of Elasticity* **2**, 1–5. Thermoelasticity.
6. A. E. GREEN and P. M. NAGHDI 1991 *Proceedings of the Royal Society of London Series A*. **32**, 171–194. A re-examination of the basic postulate of thermodynamics.
7. A. E. GREEN and P. M. NAGHDI 1992 *Journal of Thermal Stresses* **15**, 253–264. On undamped heat waves in an elastic solid.
8. A. E. GREEN and P. M. NAGHDI 1993 *Journal of Elasticity* **31**, 189–208. Thermoelasticity without energy dissipation.
9. A. C. ERINGEN 1970 *Course of Lectures*, vol. 23, CISM Udine. Berlin: Springer, Foundation of micropolar thermoelasticity.
10. W. NOWACKI 1966 *Proceedings of IUTAM Symposia*, 259–278. Couple Stresses in the Theory of Thermoelasticity.
11. R. S. DHALIWAL 1971 *Archives of Mechanics* **23**, 705–714. The steady-state axisymmetric problem of micropolar thermoelasticity.
12. R. KUMAR, T. K. CHADHA and L. DEBNATH 1987 *International Journal of Mathematics and Mathematical Science* **10**, 187–198. Lamb's plane problem in micropolar thermoelastic medium with stretch.

13. R. KUMAR and B. SINGH 1996 *Proceedings of the Indian Academy of Science* (*Mathematical Science*) **106**, 183–189. Wave propagation in a micropolar generalized thermoelastic body with stretch.
14. M. U. SHANKER and R. S. DHALIWAL 1975 *International Journal of Engineering Science* **13**, 121–128. Dynamic coupled thermoelastic problems in micropolar theory—I.
15. A. C. ERINGEN 1968 *Theory of micropolar Elasticity in Fracture*, Vol. II. New York: Academic Press, Chapter 7.
16. G. HONIG and V. HIRDES 1984 *Journal of Computational and Applied Mathematics* **10**, 113–132. A method for the numerical inversion of the Laplace transform.
17. W. H. PRESS, S. A. TEUKOLSKY, W. T. VELLERLING and B. P. FLANNERY *Numerical Recipes*. Cambridge: Cambridge University Press, 1986.
18. A. C. ERINGEN 1984 *International Journal of Engineering Science* **22**, 1113–1121. Plane waves in non-local micropolar elasticity.